

RF INJECTOR BEAM DYNAMICS OPTIMIZATION FOR LCLS-II *

C.F. Papadopoulos †, D. Filippetto, F. Sannibale, LBNL Berkeley CA, 94720
P. Emma, T. Raubenheimer, J. Schmerge, L. Wang, F. Zhou, SLAC, Menlo Park CA, 94025

Abstract

LCLS-II [1, 2] is a proposal for a high repetition rate (>1 MHz) FEL, based on a CW, superconducting linac. The LCLS-II injector is being optimized by a collaboration from Cornell University, Fermilab, LBNL, and SLAC. There are a number of different possible technical choices for the injector including an rf gun or a high voltage DC gun. In this paper we present the status of the simulations for the injector optimization for an rf gun choice for LCLS-II. A multiobjective genetic optimizer is implemented for this reason, and optimized solutions for different bunch charges, corresponding to different operating modes, are presented. These operating points are also the initial part of the start-to-end simulations for LCLS-II. Finally, we discuss the trade-offs between compression and brightness conservation in the low energy (<100 MeV) part of the accelerator, as well as the status of sensitivity studies.

INTRODUCTION

The injector is the low energy (<100 MeV) part of the accelerator, where space charge effects and non-relativistic kinematics play an important and even dominant role. Indeed, from a physical point of view, the injector ends when these effects are said to be frozen in, meaning that they no longer dominate the dynamics.

In the current paper, we describe the simulation studies and numerical optimization procedure for the injector of the LCLS-II linac-based FEL. For this, three different modes of operation are discussed, corresponding to three different bunch charges, namely at 100 pC (the baseline) as well as 20 pC and 300 pC. The code used to model the beam at the relevant regime is ASTRA [3].

The design of the injector is based on the APEX photoinjector experiment at LBNL [4].

INJECTOR OPTIMIZATION GOALS

The most fundamental requirement at the exit of the injector is a high brightness electron beam. This, especially for FEL applications, is taken to mean the 6D brightness of the beam, which is quantified by $B_{6D} = Q/(\epsilon_{nx}\epsilon_{ny}\epsilon_{nz})$, where Q is the bunch charge and the ϵ_n quantities refer to the normalized emittances in the respective planes.

In addition to this, FEL operation requires high peak current per bunch (≈ 1 kA) and correspondingly short bunches (in the order of few tens fs or less) at the exit of the linac. Since beams with this short length and the required charge

and brightness cannot be created at the cathode, compression is needed downstream. Hence, a trade-off between compression at the injector and compression at the downstream linac exists. Finally, in all three of the bunch charges cases, a laser heater is operated at the injector exit in order to increase the slice energy spread of the beam and avoid microbunching during compression. Due to this, the 6D brightness of the beam is reduced artificially at the injector exit, to avoid a larger, uncontrolled increase downstream.

Putting all this together, the two main objectives at the injector exit are the transverse emittance of the beam and the bunch length. Since for the purposes of this study we will focus on cylindrically symmetric effects, and to first order this symmetry is not broken in the injector, we can use the emittance in one plane (in our case ϵ_{nx}) as the first objective and the rms bunch length (σ_z) as the second one. Effects that break this symmetry, such as dipole and quadrupole modes due to asymmetric RF couplers are reported separately.

In addition to minimizing the emittance and the bunch length, there are certain constraints that need to be met at the injector exit. Namely, we have that a) total energy > 90 MeV, b) correlated rms energy spread < 1% (in order to accommodate the energy acceptance of the laser heater) and c) high order, correlated momentum spread $\sigma_{pHO} < \sigma_{max,Q}$, where $\sigma_{max,Q}$ is a limit that depends on the downstream compression, which is different for different bunch charges.

The high order momentum spread is defined by the relation $\sigma_{pHO}^2 = \langle p_{HO}^2 \rangle$, where the momentum p_{HO} is constructed from the original momentum distribution $p(z) = p_0 + c_1z + c_2z^2 + O(z^3)$. The variable z refers to the longitudinal position in the bunch and p_{HO} is given by the $p_{HO} = O(z^3)$ terms. Physically, this can be justified since the p_0 term is the average momentum which doesn't affect beam brightness, and the terms corresponding to c_1 and c_2 can be removed by dephasing the downstream linac and by using a third harmonic cavity downstream respectively. Both of these are standard practices in linac driven FEL facilities. The precise value of the limit imposed on σ_{pHO} depends on the downstream linac dynamics [5], but the empirical values we use are 2, 10 and 15 keV/c for the 20, 100 and 300 pC respectively.

BOUNDARY CONDITIONS

For the purposes of this study, the basic components of the injector are being kept at constant locations. A conceptual schematic of the injector, which includes only the most important elements from a beam dynamics perspective is shown in Fig. 1.

In addition to this, some of the assumptions we make that are the same for all optimization runs are given below. The initial thermal emittance coefficient of the beam at the cath-

* This work was supported in part by the Work supported, in part, by the LCLS-II Project and by the Director of the Office of Science of the US Department of Energy under Contract no. DEAC02-05CH11231

† cpapadopoulos@lbl.gov

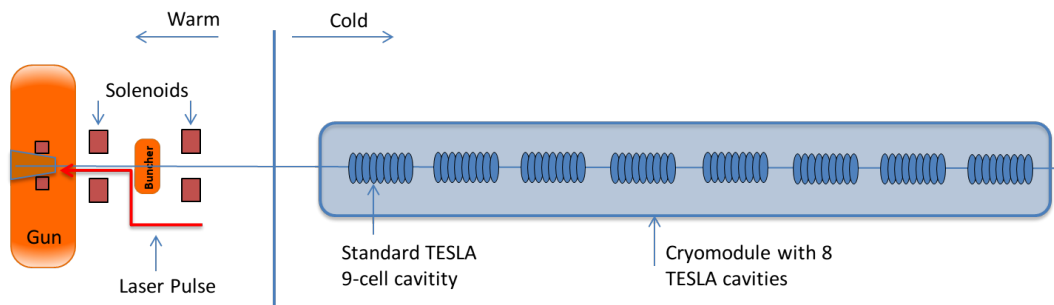


Figure 1: Schematic of the LCLS-II injector. Note the normal conducting gun and buncher and the cold, superconducting part of the injector after the focusing solenoid.

ode is 1 mm-mrad/mm, which is a conservative estimate of the real value corresponding to Cs_2Te photocathodes. The initial laser pulse transverse shape at the cathode is a radially uniform distribution. Operational experience and theoretical analysis [6] indicate that a 2-dimensional Gaussian distribution leads to smaller emittance growth downstream. Since this mode of laser shaping is also more efficient from an operational point of view, future simulations and operation of the injector will include this. The initial laser pulse longitudinal shape is a plateau with rise and fall time of 2 ps. This is consistent with the method used experimentally to give the desired bunch length (pulse stacking). Since the rise and fall time is much smaller than the plateau values, the RMS bunch length will be very close to the plateau value divided by $\sqrt{12}$. For the photocathodes used, the laser profile corresponds very well with the electron beam profile at the cathode, and only the latter is used in the simulations.

The bucking coil before the cathode is typically used to cancel the effect of the magnetic field of the 1st solenoid at the cathode. In the current layout, the effect of this in the beam emittance is calculated to be very small and the bucking coil is switched off.

OPTIMIZER DESCRIPTION

A multi-objective genetic optimizer based on the NSGA2 algorithm is used to perform the beam dynamics optimization [7,8]. The result of this procedure is not a single solution, but a “Pareto front” of multiple solutions. For the purpose of start-to-end simulations, one such solution is picked for each of the 3 charge cases. The knobs used in this optimization procedure are given in Table 1, which also describes briefly their function.

It should be noted though that due to the intensity of space charge in the injector, most of these knobs are nonlinearly coupled. In the case of the 100 pC case, the optimization procedure is allowed to have 3 additional knobs, namely the phase of the buncher cavity and the phases of the 1st and 2nd TESLA cavities. In addition to this, a 3rd objective was used, the skewness of the longitudinal distribution at the injector exit. The resulting values for those 3 phases were very close to zero crossing for the buncher and on-crest acceleration for the 2 TESLA cavities, and it was decided to simplify

Table 1: Knobs used for injector optimization. All cavity fields refer to on-axis, peak electric field. Phase of 0 is taken to mean peak acceleration and -90 is zero crossing.

| Knob | Value | Function |
|------------------------------|-------------|--------------------------------------|
| Gun Phase | -15-15 deg | Controls initial bunch length |
| Buncher field | 0-4 MV/m | Compression, Emit. comp. |
| Sol 1 B field | 0.01-0.2 T | Emit. comp. |
| Sol 2 B field | 0.01-0.2 T | Emit. comp. |
| CAV 1 field | 5-25.8 MV/m | Emit. comp. |
| CAV 2 field | 5-25.8 MV/m | Emit. comp. |
| RMS spot size at the cathode | 0.05-2 mm | Control initial space charge effects |
| Bunch length at cathode | 10-60 ps | Control initial space charge effects |

the optimization procedure and set those 3 phases to the corresponding constant values. Doing this, the skewness of the distribution was improved and the 3rd objective of skewness was also removed, significantly improving the convergence time of the optimizer. In the case of 100 pC, the optimized solution is based on the first approach, whereas for the 20 and 300 pC cases the optimized solutions are based on the second approach. Finally, once the optimizer is converged, one of the optimized solutions from the Pareto front is chosen, and is run with higher accuracy, typically 250000 particles and a grid of 75×130 , for the radial and longitudinal directions respectively. This is done both to minimize numerical errors in ASTRA simulations and in order for the particle distribution to be used downstream in linac simulations.

DISCUSSION OF OPTIMIZED SOLUTIONS

For the 100 pC case, a combined plot of the main beam phase space cuts and projections is given in Figure 2. We note that the beam slice emittance is always lower than the value of the projected emittance, as is typical. In addition to this, the 95% emittance, in which case the outer 5% of

Content from this work may be used under the terms of the CC BY 3.0 licence (© 2014). Any distribution of this work must maintain attribution to the author(s), title of the work, publisher, and DOI.

particles in 4D ($x, x\dot{z}, y, y\dot{z}$) space is ignored in the calculation, is significantly lower than the full number. The requirements on emittance for the 20 pC, 100 pC and 300 pC are 0.2 mm-mrad, 0.45 mm-mrad and 0.7 mm-mrad respectively.

The mismatch parameter ζ is defined for each longitudinal slice by the equation $\zeta_i = \frac{1}{2} (\beta_i \gamma_0 - 2\alpha_i \alpha_0 + \beta_0 \gamma_i)$ where α , β and γ are the usual Courant-Snyder parameters, for the specific slice with index i and the reference with index 0. The reference can be either the slice corresponding to the peak current value, or, as in our case, the average functions for the projected beam. The ideal value, for the case of a perfectly matched beam, is 1.

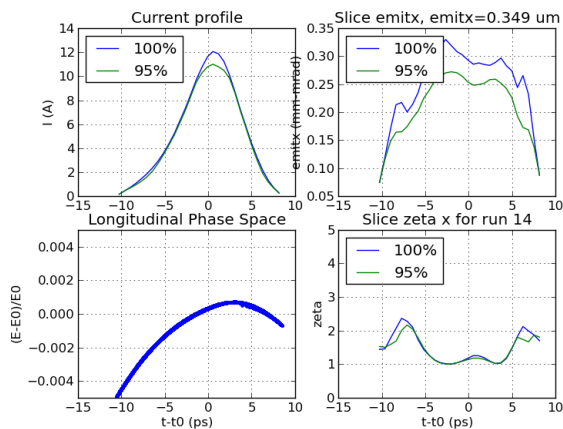


Figure 2: Optimized solution for 100 pC bunch charge, corresponding to the baseline LCLS-II design. The slice emittance is below 0.45 mm-mrad

For 20 pC, the optimized solution is shown in Fig. 3.

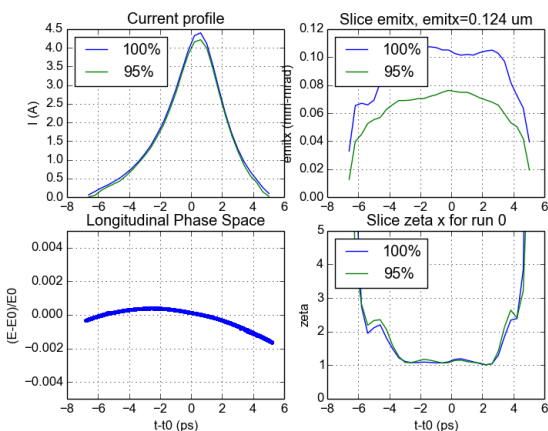


Figure 3: Optimized solution for 20 pC bunch charge. The slice emittance is below 0.2 mm-mrad

Finally, for 300 pC, the optimized solution is shown in Fig. 4.

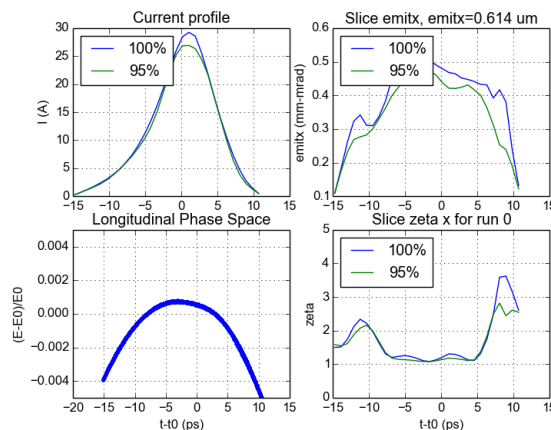


Figure 4: Optimized solution for 300 pC bunch charge. The slice emittance is below 0.7 mm-mrad

CONCLUSION

We discuss the optimization procedure and the optimized solutions for three different operating charges for a possible design of the LCLS-II injector based on a normal conducting RF gun. In all the cases discussed, simulations show that an injector based on the APEX project at LBNL meets the specifications, which are given primarily through the slice emittance at different operating charges (100 pC, 20 pC, 300 pC). Downstream linac simulations are reported elsewhere [5].

Finally, we should add that further optimization of the injector setup is possible by modifications in the number and positions of different elements. This is currently under evaluation.

REFERENCES

- [1] The LCLS-II Collaboration. "LCLS-II Conceptual Design Report". Technical report, 2013.
- [2] J. Galayda et al., "The LCLS-II Project", Proc. of IPAC'14, TUOCA01, 2014.
- [3] K. Flöttmann, "ASTRA: A Space Charge Tracking Algorithm", user's manual available at http://www.desy.de/~mypyflo/Astra_dokumentation
- [4] D. Filippetto et al., "Status of the APEX Project at LBNL", Proc. of IPAC'14, MOPRI054, 2014.
- [5] L. Wang et al., "Multi-objective Genetic Optimization for LCLS-II X-Ray FEL", Proc. of IPAC'14, THPRO037, 2014.
- [6] F. Zhou et al., "High-brightness Electron Beam Evolution Following Laser-Based Cleaning of a Photocathode", *Phys. Rev. ST Accel. Beams*, 15:090703, Sep. 2012.
- [7] Ivan V. Bazarov and Charles K. Sinclair, "Multivariate Optimization of a High Brightness DC Gun Photoinjector", *Phys. Rev. ST: Accel. Beams* 8(3):034202+, Mar. 2005.
- [8] K. Deb, "Multi-Objective Optimization using Evolutionary Algorithms", Wiley 2001.